ISSN: 2182-2069 / E-ISSN: 2182-2077

Detecting Conjunctival Hyperemia Using an Effective Machine Learning based Method

S. Bamal[1*], and L. Singh[2]

[1*]Research Scholar, School of Engineering & Technology, Sushant University, Gurgaon, Haryana, India. savitabamal85@gmail.com, https://orcid.org/0009-0002-3141-7821

[2]Professor, School of Engineering & Technology, Sushant University, Gurgaon, Haryana, India. duhanlatika@gmail.com, https://orcid.org/0000-0003-0598-6203

Received: July 22, 2024; Revised: September 2, 2024; Accepted: October 2, 2024; Published: November 30, 2024

Abstract

Among the many complex sensory organs, the human eye stands out. Prevention of eye illnesses is of the utmost importance since irreversible vision loss might result from postponed treatment. Therefore, to manage the continuous course of eye illnesses, early identification and monitoring are vital. Hyperemia, or redness, from increased blood flow, is one sign of conjunctivitis, an eye disorder defined by inflammation of the conjunctiva. Many illnesses and problems are often curable or significantly reducible with the help of the greatest medicines, sophisticated procedures, and early, accurate diagnosis by medical experts. Because there is a severe lack of diagnostic specialists, patients with vision difficulties are often not given the care they need because their conditions are not properly diagnosed. Segmentation approaches are crucial for detecting and quantifying hyperemic areas, which are necessary for diagnosing and evaluating conjunctivitis. This paper presents a very efficient machine learning framework for the detection of eye problems. The system does this by integrating segmentation approaches with feature extraction techniques. The use of the discrete cosine transform (DCT) generates feature vectors from the segmented regions of interest. Random forests and neural networks are two machine learning classifiers that are learned using feature vectors. This approach has a 96% success rate and has potential to assist ophthalmologists in assessing the severity of illnesses in objective and accurate manner. This strategy might be advantageous for adopting ICT-based solutions in public health systems in remote regions.

Keywords: Random Forest, Segmentation, Feature Extraction, Morphological Operation, Conjunctival Hyperemia, Machine Learning.

1 Overview

One must take precautions to shield their eyes against diseases and conditions that, if untreated, will cause permanent harm to their eyes and vision. Managing the course of eye illnesses and avoiding unforeseen effects requires early recognition and monitoring of these conditions (Singh & Mittal, 2014). When blood flow is increased to a certain organ or tissue, it causes the region to become red and heated; this condition is known as hyperemia. Hyperemia may have several causes. Hyperemia is often caused by either acute or chronic situations (Lens et al., 2008). One of the first symptoms of the

Journal of Internet Services and Information Security (JISIS), volume: 14, number: 4 (November), pp. 499-510.
DOI: 10.58346/JISIS.2024.I4.031

*Corresponding author: Research Scholar, School of Engineering & Technology, Sushant University, Gurgaon, Haryana, India.

illness is a reddening, burning, or tearing of the sclera. The severity of the infection may be determined by the number of the red lesions as well as the space that they occupy (Figure 1).

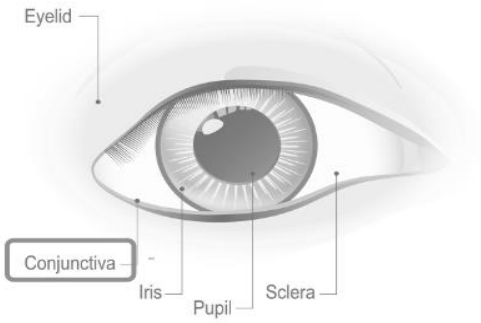

Figure 1: Image of Eye with Conjunctival

Exclusion of other possible reasons, such as allergies, dry eye, contact lens issues, or hyperemia (called erythema or conjunctival injection) (Schulze et al., 2007; Fieguth & Simpson, 2002), requires a comprehensive evaluation. Analyzing the rate of development and response to treatment is very important. Effective treatment and preservation of vision depend on early detection of conjunctivitis. There is a significant imbalance in the population-to-ophthalmologist ratio in developing countries such as India. In rural regions, the ratio is 1:219000, while in urban areas it drops to 1:25000 (Singhal et al., 2024). Due to the difficulty in providing healthcare to large populations caused by a lack of practitioners, residents in rural regions sometimes disregard health problems in their early stages (Sofiene et al., 2023). With the help of new technologies, screening problems such as conjunctiva hyperemia may soon be a thing of the past. It is suggested to use machine learning (ML) to develop a dependable model for the detection of eye diseases (Alamer et al., 2023). The method begins with segmentation to identify the specific region of interest, followed by feature extraction to collect ocular particulars, and ultimately, training a supervised learning algorithm to develop the model.

First, segmentation must be used to identify infected and healthy eye regions (the "region of interest"), and then we'll use feature extraction and machine learning techniques to separate the two. Transformation-based feature extraction method (DCT) is used on the photos. Furthermore, suitable ML methods, such as Neural Net (NN) and Random Forest (RF), are used in conjunction with k-fold cross-validation. In the beginning, segmentation methods try to use different image processing techniques to draw lines and extract the hyperemic conjunctiva utilizing the reddish hue of the conjunctiva as a distinguishing feature in comparison to healthy eye regions in pictures. By dividing the hyperemic regions into segments, it becomes possible to do more traditional testing and measurement. This includes assessing the severity of the condition by examining the degree of redness or estimating the fraction of the conjunctival area affected by hyperemia. ML methods may be used to extract the features of the target regions as an alternative during the training of the model. Machine learning methods have shown high accuracy in detecting eye-related problems and have the capacity to be more robust. Furthermore, these methodologies may be used to design devices that can effectively address public health care shortages.

The remaining sections of the document are organized as follows: Section 2 provides related works. The proposed work is outlined in Section 3. Section 4 of this paper outlines the procedures for extracting features from segmented images using the Discrete Cosine Transform (DCT) method. Neural Networks and Random Forests are both classifiers that are mentioned in Section 5. The details

and precise measurements of the achieved precision are further upon in Section 6. In the last section, the scope of the future paper is discussed.

2 Related Work

Computer aided diagnosis continues to be a subject of ongoing paper. This section is a literature review that provides a concise overview of the research conducted on computer-based systems for detecting eye redness caused by hyperemia. Prior research has established clinical and grading scale techniques for diagnosing sick eyes (Narasimha-Iyer et al., 2006). However, it is shown that these procedures are excessively time-consuming due to their manual nature. Scientists have suggested many manual and semi-automated methods to identify red lesions (Wolffsohn & Purslow, 2003; Alamer et al., 2023). Canny edge detection is a semi-automatic method that mimics the human eye's redness grading ability (Dülger & Dülger, 2022). This method divides the sclera region using segmentation. Although pixel-based repetition has its uses, the computational overhead is a major concern in some cases (Schulze et al., 2007). The image's edges are detected using a fuzzy Canny approach (Fieguth & Simpson, 2002; Singhal et al., 2024), and then morphological procedures are performed for segmentation to improve the findings (Singhal et al., 2024). A different research conducted picture analysis using a Bayesian classifier, with a specific emphasis on two main factors: the presence of redness and the visibility of blood vessels (Wang et al., 2016).

Khan, (2013) developed a computer vision system that was both costly and complex for the purpose of detecting diseases via ocular scanning. Zhou et al., (2013) came up with a complete way to rate the quality of pictures of the sclera for identification reasons. The efficacy of sclera identification may be enhanced by using several directional Gabor filters to improve the sclera vein pattern. Kaya et al. Kaya et al., (2010) showed a way to make designs more stable in laser eye surgery. This method tracked the pattern of red spots in the patient's eye by looking at features found in blood vessels in the sclera (Laddi & Kumar, 2014). The Hough transform and the RANSAC algorithm are used to make a mask that shows the ablation pattern correctly. Additionally, the SIFT approach is employed on the whole picture to decrease the number of significant points and eliminate any edge-related artifacts. Wu and Harada introduced methods for extracting blood vessels from pictures of the sclera and conjunctiva. The researchers proposed a novel technique for removing noise by using a unique pseudo vessel elimination methodology. Otsu's method is used to figure out the cutoff number on their own (Otsu, 1979).

The use of machine-learning techniques to analyze patient data on refractive error resulted in the development of a two-step diagnostic procedure. The findings indicated that tree-based approaches outperformed artificial neural networks using various methods of segmentation (Rother et al., 2004). The paper discovered a obvious relationship between the quantity of accessible data and the effectiveness and accuracy of the programs. The first paper used ICD-10 diagnostic information and deemed the most precise due to its extensive access to a substantial volume of data (Umayalakshmi, 2014). The second- and third-level assessments are then made, it is not quite as accurate. Even though the random forest method did better than the artificial neural network, it took a little longer to run than the decision tree method (Malik et al., 2019). This paper specifically looks at the methods by looking at different combos of picture characteristics to find the most important ones using feature selection methods. It has effectively decreased the collection of features from 25 to 2-3 values. Based on the Efron scale, the MLP classifier had the lowest error rate while using the features chosen by the CFS technique. According to the CCLRU scale, the MLP had the smallest error while employing the features chosen with the M5 wrapper (Brea et al., 2016).

Rigid segmentation is fundamental to the development of effective screeners. It is possible that the proposed ML model for conjunctivitis categorization represents a significant improvement in the reliability of machine-based automated screening approaches. While this study is encouraging, further research is needed to find a trustworthy and objective way to measure conjunctival hyperemia. To fill this knowledge gap, our work extracts characteristics from region of interest (ROI) photos and trains machine learning algorithms to distinguish between healthy and conjunctivitis-affected eyes. The procedures used to create this work are detailed below.

3 Proposed Method

The process workflow of the recommended technique for segmentation and classification is shown in the form of a flowchart in Figure 2, which illustrates the steps involved in the workflow. This process is dependent on algorithms that are used for machine learning.

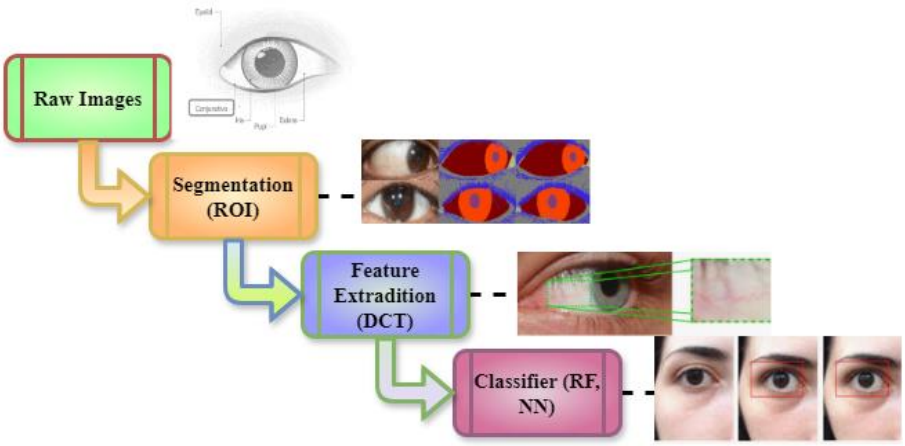

Figure 2: Proposed Methodology of Discrete Cosine Transform

An efficient model for screening eye illnesses is being developed in this research, and one of the main components of that model is image segmentation. There are a total of fifty images that are used in this article to illustrate bulbar redness, and thirty photographs are used to illustrate healthy eyes. This collection of photographs was obtained from the vision lab located inside the School of Health Sciences. The HUVITZ 500N slit light and the CANON EOS 1300D camera, both of which are integral components of the system, are used to capture the photographs. There is a three-step process involved in the acquisition technique. Examples of pictures are shown in Figure 3.

$$efh(v, Q) = j(n, q) = tjhp\left(efh * n'(q)\right) \quad (1)$$

The high blood pressure identification $n'(q)$ efficiency of feature extraction is represented by the equation (1), efh. Features vectors and segmented characteristics are described by the variables v, Q and $j(n, q)$, while the connection between a function and those variables is described by $tjhp$ and efh.

Figure 3: Diseased Eye Image and Healthy Eye Image

The illness known as hyperemia conjunctivitis requires the examination of red lesions that are located on the sclera. Figure 4 illustrates the technique that is described, and the flowchart provides more explanation.

$$esp(m, Q) = rsp(z', V_2) * esp\ (m^2, R_2)\ (2)$$

Here, $esp\ (m^2, R_2)$ symbolizes the efficiency of extraction of features with lined factors $rsp(z', V_2)$ indicates the reaction of the method of segmentation concerning the divided regions, as well as the function $esp(m, Q)$, indicates the efficacy of dividing and removing features in Equation (2).

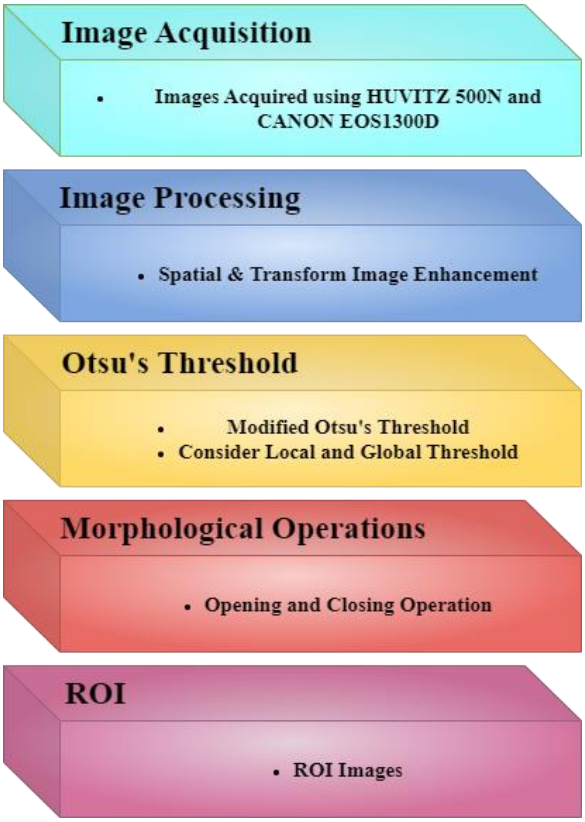

Figure 4: Visualization of the Suggested Segmentation Procedure

The images are acquired by hand, thus preprocessing techniques are used to remove any noise or extraneous areas that aren't necessary for disease grading. Image cleaning often makes use of spatial and transform-based techniques. Changing the values of individual pixels is the mainstay of spatial domain methods for image improvement. This paper explores two methods: histogram equalization and contrast stretching. When the background and foreground are both quite bright, histogram equalization—which increases visual contrast by spreading out shared intensity values—work wonders on the image. Because it increases the dynamic range of the picture, contrast stretching improves it. The equation is given below:

Most people agree that Otsu's thresholding approach is the best option most of the time (Singhal et al., 2024). Using a tweaked version of Otsu's thresholding method, we can get the overall threshold value for a 2D image array. This program iteratively searches for the tiniest discrepancies in variances between two pixel sets. Through repeated cycles, the algorithm aims to find the cutoff that, for each class, minimizes variability. The acquisition of the ideal threshold value is followed by classification

of the picture into two parts (sclera and non-sclera component). For a clearer picture, see Figure 5, where the left side shows the original matrix and the right side shows the output using Otsu's technique.

$$\forall_{N*Q} = \{(q,r) \equiv N * K : (0,q,r) \equiv \forall(D-1)\} \quad (3)$$

The removal of features and segmentation method is represented by the pair of parameters (q,r) in the equation $\forall_{N*Q}$ where K acts as scaling factors and $D-1$ is the data dimension in question. The aforementioned requirements N are guaranteed to be satisfied by the settings q and r for every single value within the required range $\forall_{N*Q}$ according to this equation (3), which guarantees accurate swelling detection $\forall$ via consistent delineation and extracted features.

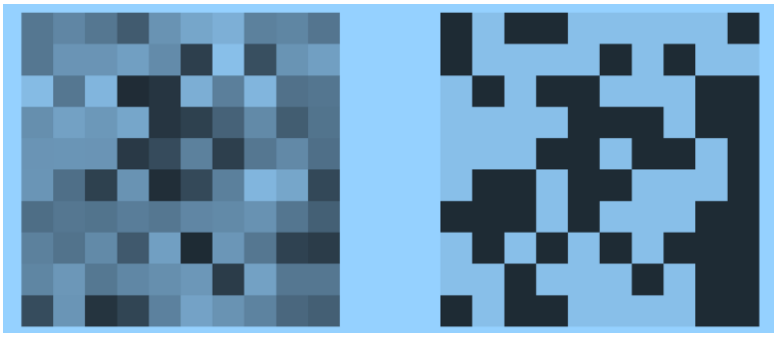

Figure 5: LHS-Original Matrix and RHS Segment Scale Color

The final picture is then processed using morphological techniques to make the segmentation findings even more precise. Figure 6 shows the accurate procedures used in the morphological processes.

$$\{(0,q,r) \equiv [0,\forall] \times D_f\ (N \times W) : (q,r) \equiv n^{-1}(0) \geq \propto_{N*Q}\} \quad (4)$$

The standardization or factor of scaling is represented by $n^{-1}(0)$ in the equation (4), and it additionally shows the starting parameters as $(0,q,r) \equiv [0,\forall]$ and the data dimensionality and the space of features as $D_f\ (N \times W)$. The feature vectors must fulfill the necessary criterion to effectively classify and accurately identify conjunctive high blood pressure, which is $\propto_{N*Q}$.

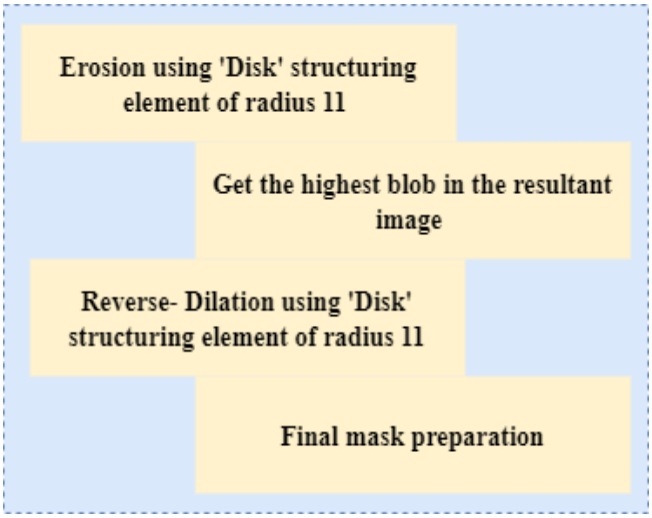

Figure 6: Morphological Operations Steps

To evaluate the accuracy of the suggested technique, Figures 7 and 8 show the raw photos and comprehensive sample segmented ROI findings of fifty photographs.

$$y = p * g(v, e), or\ z = h(r) + \partial m(v, k) \quad (5)$$

The system's ultimate output is represented by the equation (5), y, where $p * g(v, e)$ is a function that might be related to feature extractor or classifications and involves inputs z and $h(r)$. Another possible output, denoted as ∂m, may be defined as the sum of v and k, where reflect extra stages in filtering or adjustment.

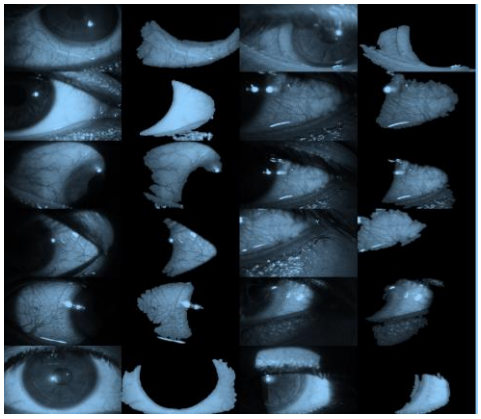

Figure 7: Segmented (ROI) Result Images

The image depicts a series of segmented regions of interest (ROIs) from close-up images of eyes, likely intended for medical or computer vision analysis. Each column shows a sequence of eye images, with corresponding segmented areas isolating specific anatomical features, such as the cornea or sclera. The segmentation likely highlights regions critical for tasks like diagnosing eye conditions, tracking eye movements, or other vision-related research. The monochromatic blue tint adds a clinical and precise feel to the images, emphasizing the importance of these segments in detailed analysis, potentially for machine learning or medical diagnostics.

$$|g(u, q_1, p_2) - g(v, q_r, m_{n-1})| \geq (|\partial_1 \times \partial_2|) \quad (6)$$

Two functions that reflect the outcomes of extraction of features or classifying with distinct parameter sets are $g(u, q_1, p_2)$ and $g(v, q_r, m_{n-1})$. By comparing this variation to the result of parameters ∂_1 and ∂_2, the inequality verifies that the model created using machine learning is successful and reliable in identifying conjunctive elevated blood pressure in equation (6).

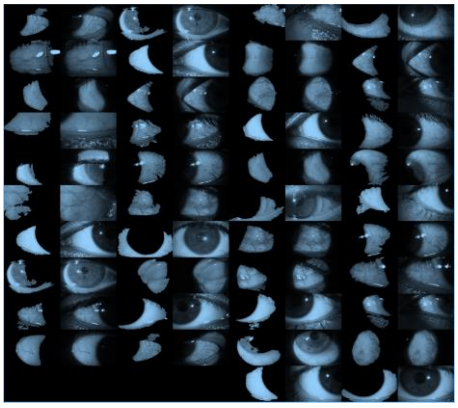

Figure 8: Image Showing ROI

Figure 8 illustrates a collection of eye images paired with their corresponding regions of interest (ROIs). The image is organized in a grid format, where each eye image is followed by its segmented ROI, likely focusing on critical features like the cornea or sclera. The monochromatic blue color scheme adds a clinical atmosphere, emphasizing the precision and importance of these segments for analysis. This figure is likely used in medical research, eye-tracking studies, or machine learning models for eye-related diagnostics, highlighting the segmented areas essential for accurate assessment and further investigation.

$$f_w\big(u, q_{w-1}, r, \propto (p-1)\big) \rightarrow g\big(u, q_0, e, \propto_{1-q}\big) \quad (7)$$

The feature selection function with values u, q_{w-1}, $r, \propto (p-1)$ is represented by the equation (7) f_w, and the output functional without parameter u, q_0, e, and $\propto_{1-q}$ is denoted by g. The transformation of the original characteristics and attributes through the equipment to produce the final output is shown by this equation for analysis of accuracy with NN and RF.

$$m^{-2}(2) \equiv \forall_{N-M} = m^{-1}(2) \equiv R_0 = h^{-1}(1) \quad (8)$$

Different degrees of variable scaling linked to feature extraction $\forall_{N-M}$ are represented by the equations (8), $m^{-2}(2)$ and $m^{-1}(2)$, with R_0 denoting a particular reference or threshold amount. The characteristics vectors can be normalized and expanded consistently since the limit is in alignment with the transformed functioning.

4 Classification and Feature Extraction

Important patterns or features may be highlighted by feature extraction, a critical step in machine learning that entails extracting and manipulating pertinent data from a dataset. Imaging ROIs of healthy eyes compared to conjunctivitis photos yields more accurate results. In sections 4.1 and 4.2, the procedures are detailed.

4.1. Feature Extraction of ROI Images Using DCT Transformation

The Discrete Cosine Transform (DCT) is a way to depict a picture by dividing it into many sinusoidal components with different widths and frequencies. The DC coefficients are shown to the right of the first black block in the illustration. The 2-D DCT transformation accurately captures the picture's visually key properties using DCT cosine coefficients.

Next, training subset is used to teach the classifier, allowing it to understand the relationships and patterns between the DCT characteristics and their respective classes. The testing subset is used to evaluate the classifier's performance after the training phase. Measures such as recall, accuracy, and precision are used for model improvement and evaluating classification performance. When trained to meet the requirements of its design, a neural network employs a series of successive neural layers. Using a learning rate of 0.1, the model is assessed over 50 iterations using the suggested neural net classifier.

The use of the random forest method to construct decision tree classifiers is another typical classifier outcome. Each tree has its own unique data gathering mechanism to generate a random vector. Every tree vector created randomly adheres to the same probability distribution.

5 Result and Discussion

Performance Metrics

At each stage of the categorization process, three performance metrics are monitored: accuracy, precision, and recall. Popular recall, accuracy, and precision metrics are used to evaluate the ML algorithms' output. These measurement indices are in various previous research, such as [15]. The diseases are categorized as either positive or negative in a normal situation.

This approach utilizes the frequency information provided by the DCT characteristics to identify hyperemic areas or other segmented regions of interest in photos.

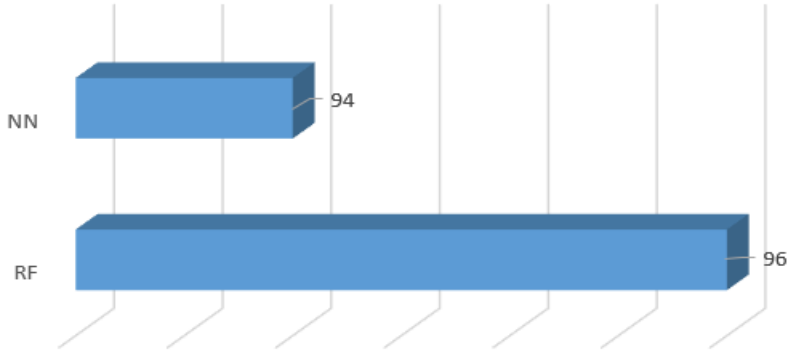

Figure 9: Analysis of Accuracy with NN and RF

Figure 9 shows a comparison of the accuracy of two machine learning models: Random Forest (RF) and Neural Network (NN). The graphic clearly demonstrates that the Random Forest model outperformed the Neural Network model, which only managed 94% accuracy. The Random Forest model obtained an impressive 96% accuracy. The 3D bar layout draws attention to the disparity in performance, drawing attention to the Random Forest model's higher accuracy. To choose the best model for machine learning tasks like classification, prediction, or any other application, this visual depiction is helpful for comparing the efficacy of several methods. Figure 10 and the accompanying bar graphs illustrate the outcomes of a thorough comparison of accuracy with and without ROI on raw photos.

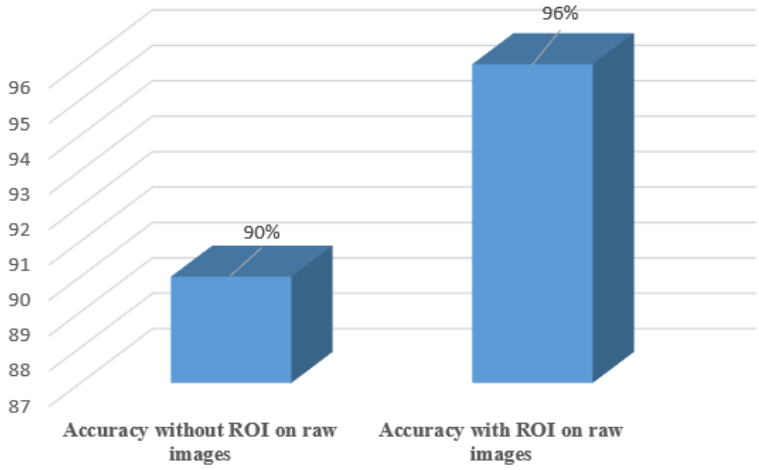

Figure 10: Analysis of Comparison of Results with or Without ROI on Raw Eye Images

Using images captured locally using the slit lamp method, the classifier is trained and measured. After the images have been segmented using morphological methods, DCT is used to obtain the feature vector from the ROI images. Classifiers learn to differentiate between the two classes using this extracted feature vector as a training input. Fifty images of sick people and thirty images of healthy ones make up the dataset used to test the suggested model. When doing the assessment, random forest and neural networks are used as classifiers. The neural network model achieves 94% accuracy, whereas the random forest technique reaches 96% precision. As shown in Figures 9 and 10, the Random Forest achieves the best accuracy (96%) with 50 features, out of all the features currently available.

6 Conclusion

Machine learning (ML) models built on image processing may reliably detect hyperemia conjunctivitis, defined by erythema and edema of the conjunctiva. In this study, we use a machine learning classification technique to build a segmentation model that can detect conjunctiva hyperemia and other eye illnesses during screening. To improve accuracy, this method relies on feature extraction rather than using raw photos or applying algorithms to segmented images, as is the case with other image screeners. By using Otsu's thresholding and morphological approaches, one may get accurate segmentation results. Discrete Cosine Transform (DCT) coefficients were then used for feature extraction on the segmented regions. A machine learning classifier receives the feature data that has been collected. Using Random Forest and Neural Network classifiers, the proposed technique achieved an impressive 96% accuracy rate, with normal eyes achieving 87% accuracy. When compared to training on raw images without removing the target region, results obtained by segmentation and feature extraction are often superior. The findings indicate that this research has improved the accuracy of hyperemia conjunctivitis detection. A significant gain in accuracy is achieved by integrating machine learning models that use image processing, segmentation, and feature extraction methods. Improvements in the accuracy and efficiency of hyperemia conjunctivitis picture assessment and therapy are anticipated outcomes of this work.

References

[1] Alamer, L., Alqahtani, I. M., & Shadadi, E. (2023). Intelligent Health Risk and Disease Prediction Using Optimized Naive Bayes Classifier. *Journal of Internet Services and Information Security, 13*(1), 1-10. https://doi.org/10.58346/JISIS.2023.I1.001

[2] Brea, M. L. S., Barreira-Rodríguez, N., Sánchez-Maroño, N., González, A. M., García-Resúa, C., & Yebra-Pimentel, E. (2016). On the analysis of feature selection techniques in a conjunctival hyperemia grading framework. In *ESANN*, 271-276.

[3] Dülger, G., & Dülger, B. (2022). Antibacterial Activity of Stachys sylvatica Against Some Human Eye Pathogens. *Natural and Engineering Sciences, 7*(2), 131-135. https://doi.org/10.28978/nesciences.1159224

[4] Fieguth, P., & Simpson, T. (2002). Automated measurement of bulbar redness. *Investigative ophthalmology & visual science, 43*(2), 340-347.

[5] Kaya, A., Can, A. B., & Çakmak, H. B. (2010, August). Designing a pattern stabilization method using scleral blood vessels for laser eye surgery. In *2010 20th International Conference on Pattern Recognition* (pp. 698-701). IEEE. https://doi.org/10.1109/ICPR.2010.176

[6] Khan, M. W. (2013). Technology & Research Diabetic Retinopathy Detection using Image Processing: A Survey. *International Journal of Emerging Technology & Research*, *1*(1), 16-20.

[7] Laddi, A., & Kumar, A. (2014). Intelligent Machine Vision Technique for Disease Detection through Eye Scanning. *Case Studies in Intelligent Computing: Achievements and Trends*, *17*.

[8] Lens, A., Nemeth, S. C., & Ledford, J. K. (2008). *Ocular anatomy and physiology*. Slack Incorporated.

[9] Malik, S., Kanwal, N., Asghar, M. N., Sadiq, M. A. A., Karamat, I., & Fleury, M. (2019). Data driven approach for eye disease classification with machine learning. *Applied Sciences*, *9*(14), 2789. https://doi.org/10.3390/app9142789

[10] Narasimha-Iyer, H., Can, A., Roysam, B., Stewart, V., Tanenbaum, H. L., Majerovics, A., & Singh, H. (2006). Robust detection and classification of longitudinal changes in color retinal fundus images for monitoring diabetic retinopathy. *IEEE transactions on biomedical engineering*, *53*(6), 1084-1098. https://doi.org/10.1109/TBME.2005.863971

[11] Otsu, N. (1979). A Threshold Selection Method from Gray-Level Histograms. *IEEE Transactions on Systems, Man, and Cybernetics*, *9*(1), 62–66.

[12] Rother, C., Kolmogorov, V., & Blake, A. (2004). "GrabCut" interactive foreground extraction using iterated graph cuts. *ACM Transactions on Graphics (TOG)*, *23*(3), 309-314. https://doi.org/10.1145/1015706.1015720

[13] Schulze, M. M., Jones, D. A., & Simpson, T. L. (2007). The development of validated bulbar redness grading scales. *Optometry and Vision Science*, *84*(10), 976-983. https://doi.org/10.1097/OPX.0b013e318157ac9e

[14] Singh, G., & Mittal, A. (2014). Various image enhancement techniques-a critical review. *International Journal of Innovation and Scientific Research*, *10*(2), 267-274.

[15] Singhal, P., Yadav, R. K., & Dwivedi, U. (2024). Unveiling Patterns and Abnormalities of Human Gait: A Comprehensive Study. *Indian Journal of Information Sources and Services, 14*(1), 51–70.

[16] Sofiene, M., Souhir, C., Yousef, A., & Abdulrahman, A. (2023). Blockchain Technology in Enhancing Health Care Ecosystem for Sustainable Development. *Journal of Wireless Mobile Networks, Ubiquitous Computing, and Dependable Applications, 14*(3), 240-252. https://doi.org/10.58346/JOWUA.2023.I3.018

[17] Umayalakshmi, R. (2014). An Approach to Enhancement of Iris Recognition System. *International Academic Journal of Science and Engineering, 1*(1), 158–165.

[18] Wang, X. Y., Wu, Z. F., Chen, L., Zheng, H. L., & Yang, H. Y. (2016). Pixel classification based color image segmentation using quaternion exponent moments. *Neural Networks*, *74*, 1-13. https://doi.org/10.1016/j.neunet.2015.10.012

[19] Wolffsohn, J. S., & Purslow, C. (2003). Clinical monitoring of ocular physiology using digital image analysis. *Contact Lens and Anterior Eye*, *26*(1), 27-35. https://doi.org/10.1016/S1367-0484(02)00062-0

[20] Zhou, Z., Du, E. Y., Thomas, N. L., & Delp, E. J. (2013). A comprehensive approach for sclera image quality measure. *International Journal of Biometrics*, *5*(2), 181-198. https://doi.org/10.1504/IJBM.2013.052972

Authors Biography

Savita Bamal, is a Ph.D. scholar of SET at Sushant University. She is working as software developer in test engineer. She holds a master of technology in computer science from department of computer science and applications, Kurukshetra University. Her research area includes image processing, data mining and machine learning.

L. Singh, Computer science instructor and researcher with more than 15 years of experience in teaching, research and project supervision. Expertise in developing and delivering engaging lessons, creating course material and evaluating student performance. Focused on fostering a positive learning environment and helping students reach their full potential.